JOURNAL OF CATALYSIS **164,** 94–108 (1996)
ARTICLE NO. 0366

Experimental and Modeling Study of Hydrogenation Using Deuterium Step Transient Response during Ethylene Hydroformylation

Mark A. Brundage and Steven S. C. Chuang[1]

Department of Chemical Engineering, The University of Akron, Akron, Ohio 44325-3906

Received May 7, 1996; revised July 24, 1996; accepted July 25, 1996

Deuterium isotopic step tracing combined with *in situ* infrared (IR) spectroscopy was utilized to study and model the hydrogenation steps in ethylene hydroformylation on 4 wt% Rh/SiO_2 at 483–573 K and 0.1 MPa. The difference in residence times between H_2 and D_2, as well as propionaldehyde and deuterated propionaldehyde to the step switch from H_2 to D_2 and D_2 to H_2 during ethylene hydroformylation reflects the presence of an isotope effect for H_2/D_2 chemisorption and propionaldehyde formation. Compartment modeling of H_2/D_2 responses and qualitative comparison of propionaldehyde and deuterated propionaldehyde responses unravel the presence of a normal equilibrium isotope effect for H_2/D_2 chemisorption and a normal kinetic isotope effect for hydrogenation/deuteration of adsorbed acyl species. *In situ* IR coupled with deuterium transient responses shows that the reverse spillover of deuterium from Si-OD participates in the deuteration of adsorbed acyl species, suggesting that the site for deuteration of the adsorbed acyl species is located near the Rh and SiO_2 interface. Significant difference in the deuterated ethane and propionaldehyde responses suggests the different nature of either adsorbed hydrogen/deuterium or the active site for hydrogenation/deuteration of adsorbed ethyl and acyl species.

INTRODUCTION

Deuterium tracer has been extensively used to study the mechanism of catalytic hydrogenation (1–10). Most deuterium studies have utilized either batch or steady-state techniques. The rates of appearance of deuterium-containing products and deuterium location in the deuterated products obtained from these results allow identification of reaction pathways, elucidation of the nature of the catalyst surface and deuterium-containing adsorbates, and determination of the relative rates of elementary steps and isotope effects. The observed isotope effect, defined as the reaction rate with hydrogen ($\mathbf{r}_H$) divided by the reaction rate with deuterium ($\mathbf{r}_D$), has been used to elucidate the rate-limiting step in the overall sequence of hydrogenation. However, the absence of knowledge of intermediate concentration and the lack of understanding of the complicated contribution of kinetic and thermodynamic (equilibrium) isotope effects on individual elementary steps to the observed isotope effect often lead to controversial identification of the rate-limiting step (7).

The rate-limiting step of a few catalytic reactions has been identified by steady-state isotopic-transient kinetic analysis (SSITKA) (11). The technique involves (i) replacing a reactant flow by its isotopically labeled counterpart in the form of a step function to the inlet of a flow reactor and (ii) monitoring the isotopically labeled and nonlabeled reactants in the reactor effluent as a function of time. The responses of the labeled reactants and products carry mechanistic information that allows determination of intermediate coverages and rate-limiting steps. One unique feature of SSITKA is maintaining the steady-state condition for the total concentration of gaseous isotopically labeled and nonlabeled reactants and their adsorbates during either step or pulse injection (1, 11, 12). Disturbance of the steady-state resulting from isotope effect is minimal when the mass ratio of the isotope labeled and nonlabeled species approaches one. SSITKA has been extensively used to study reactions involved with $^{12}CO/^{13}CO$, $^{14}NO/^{15}NO$, and $^{12}CH_4/^{13}CH_4$ in which both isotopically labeled and nonlabeled species react at about the same rate (3, 11), producing near symmetrical responses for both isotopically labeled and nonlabeled products, as sketched in Fig. 1a. The symmetry in the rise and decay of the response is a manifestation of the lack of isotope effect.

The isotope effect mainly results from the large mass and bonding energy differences between the molecular species and its isotopic counterpart (13). Comparison of H_2 and D_2 yields a large difference in mass ratio; therefore, its isotope effect can greatly shift thermodynamic equilibrium and alter reactivity of adsorbates by varying the rates of elementary steps, upsetting the steady-state conditions for the total concentration of hydrogen- and deuterium-containing adsorbates during the step switch from H_2 to D_2 flow. Deviation from the steady-state total concentration of adsorbates resulting from the isotope effect should shift the hydrogen- and deuterium-containing product responses

[1] To whom correspondence should be addressed.

0021-9517/96 $18.00

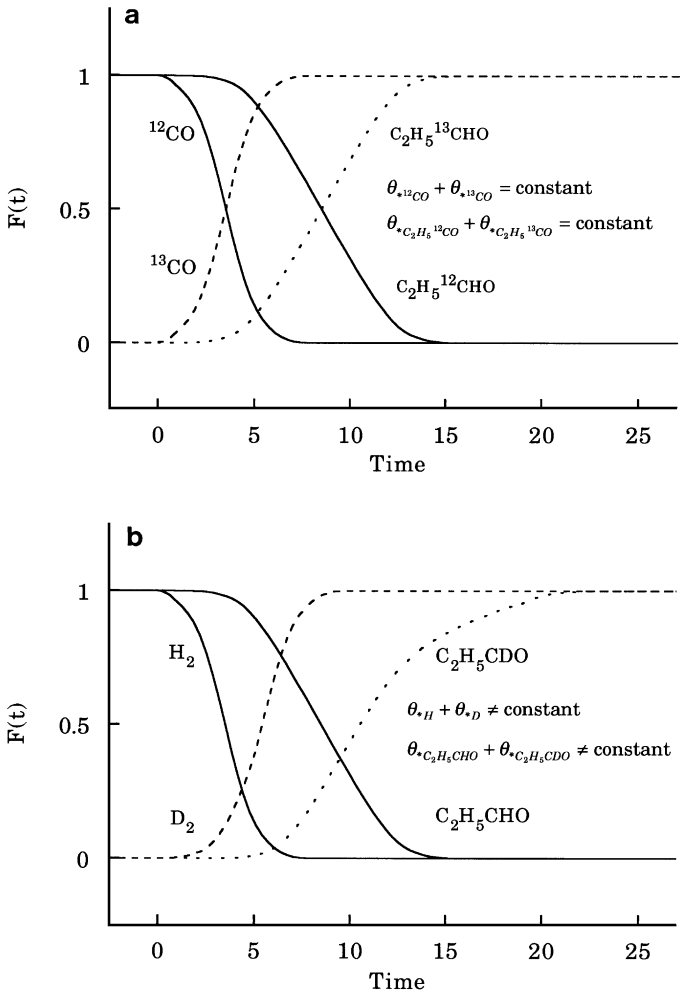

FIG. 1. (a) Propionaldehyde transient responses to a ^{12}CO to ^{13}CO step switch during $CO/H_2/C_2H_4$ reaction. (b) Possible propionaldehyde transient responses to a H_2 to D_2 step switch during $CO/H_2/C_2H_4$ reaction.

from the symmetrical form to the one shown in Fig. 1b. Modeling of both hydrogen- and deuterium-containing product responses may allow determination of the isotope effect on the coverage of intermediates and unambiguous identification of rate-limiting steps. While a number of hydrogen/deuterium step switch studies have been reported for methanation (3) and ammonia synthesis (11), the quantitative analysis of hydrogen- and deuterium-containing product responses has never been attempted due to the complexity of the isotope effect on the product responses.

This paper reports the results of a H_2/D_2 step switch study on ethylene hydroformylation on Rh/SiO_2. Hydroformylation is selected for testing H_2/D_2 isotopic transient techniques because of its industrial importance and simplicity in the product distribution. Hydroformylation is the reaction of an olefin with synthesis gas (CO/H_2) to form an aldehyde with one more carbon atom than the original olefin. The industrial hydroformylation process utilizes a homogenous catalyst, thus requiring an energy-intensive separation (14). Although a heterogeneous gas–solid hydroformylation process eliminates the separation step, the heterogeneous catalysts under investigation, including supported Rh, suffer from low aldehyde selectivity, with the majority of the product being the alkane. Figure 2 shows the proposed reaction pathway for heterogeneous ethylene hydroformylation (15, 16). The formation of both ethane and propionaldehyde involves hydrogenation reactions: (i) the hydrogenation of the adsorbed alkyl species to form ethane and (ii) the hydrogenation of the adsorbed acyl species to form propionaldehyde. The H_2/D_2 isotopic transient technique may help unravel the factors controlling the selectivity of the reaction. A fundamental understanding of the hydrogenation steps involved in the formation of alkane and aldehyde products may lead to an effective approach to suppress the hydrogenation of alkyl intermediates, thereby enhancing the aldehyde selectivity.

This study aims at investigation of the H_2/D_2 isotope effect on the coverage of intermediate and hydrogenation steps for propionaldehyde and ethane formation during ethylene hydroformylation on Rh/SiO_2. Hydrogen and deuterium as well as hydrogen- and deuterium-containing product responses were obtained by a step switch from H_2 to D_2 flow while the CO and C_2H_4 flows were maintained at steady state. The hydrogen- and deuterium-containing product responses were fit to the step response of a compartment model to obtain the coverage of intermediates and the rates of elementary steps. This study demonstrates the advantages and limitations of the step switch from H_2 to D_2 and from D_2 to H_2 techniques to investigate hydrogenation mechanism. Results of this study are compared with those of our previous ^{13}CO SSITKA study to further improve understanding of hydrogenation steps in the ethylene hydroformylation reaction.

EXPERIMENTAL

Catalyst Preparation

A 4 wt% Rh/SiO_2 catalyst was prepared by incipient wetness method. An aqueous solution of $RhCl_3 \cdot 3H_2O$ (Alfa Products) was impregnated into a large pore SiO_2 support (Stream Chemicals, surface area of 350 m^2/g). The ratio of the volume of solution to the weight of silica support used in the impregnation step was 1 cm^3 to 1 g. After impregnation, the sample powder was dried in air at 298 K overnight and then reduced in flowing hydrogen at 673 K for 16 h. The H_2 uptake of the catalyst was measured at 303 K by pulse adsorption method and was found to be 61 μmol/g, corresponding to a dispersion of 0.62 and a crystallite size of 15 Å, assuming an adsorption stoichiometry of $H_{ads}/Rh = 1$ and a cubic shape of Rh crystallites.

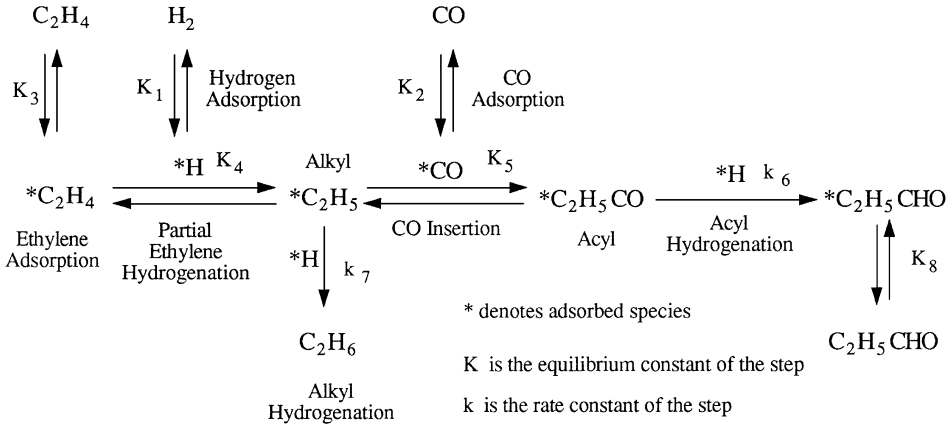

FIG. 2. The reaction pathway of heterogeneous hydroformylation.

Reaction Studies

The apparatus used in this study has been previously reported in detail (17) and will be described briefly. Approximately 80 mg of catalyst powder was pressed into five self-supporting disks. One disk was placed in the IR reactor cell beam path and the rest were broken up and placed in the outlet stream of the reactor to increase the product concentration in the effluent stream. Prior to the series of experiments, the catalyst sample was further reduced for 2 h under H_2 flow at 673 K and 0.1 MPa. Steady-state flows of H_2, CO, C_2H_4, and He at a 1/1/1/1 ratio for a total flow rate of 120 cm^3/min were controlled by mass flow controllers and were combined at a mixing point before entering the infrared (IR) reactor cell. The IR reactor cell acted as a differential reactor to obtain the initial rates for the forward reaction.

Upon reaching steady state for 30 min, the steady-state gaseous product concentrations were determined by an HP-5890A gas chromatograph (GC). The GC contains two 6-ft packed columns in series, a Poropak PS and a Poropak QS, and is equipped with a flame ionization detector (FID). The retention time and the FID response were found to be insensitive to the differences between hydrogen- and deuterium-containing C_2-hydrocarbons by injecting C_2H_4 and C_2D_4 samples and then comparing the retention times and area responses. Similar retention times and FID responses were reported for CH_4 and CD_4 (6).

Following the steady-state measurement, a 4-port valve was utilized to introduce a step switch from H_2 to D_2, while maintaining the steady-state flow rates of CO and C_2H_4, to produce transient responses of hydrogen- and deuterium-containing adsorbates and products. The H_2 flow contained 2% Ar which does not adsorb on the catalyst surface. Ar is utilized as a tracer to obtain the flow characteristics from the isotope injection point to the mass spectrometer sampling point. Subtracting the residence time of Ar from that of the product species reveals the residence time of the adsorbed intermediates.

The transient responses of the adsorbed species on the catalyst surface were monitored by the IR spectrometer. The *in situ* IR spectra are recorded using a Nicolet 5SXC spectrometer with a DTGS detector at a resolution of 4 cm^{-1} that is interfaced to a computer. Thirty-two scans are coadded when recording spectra under steady-state conditions while only four are coadded under transient conditions to facilitate rapid scanning. The transient responses of the gaseous products from the IR cell were recorded by a Balzers QMG 112 mass spectrometer (MS) that is interfaced to a computer. The MS is equipped with a differentially pumped inlet system located directly downstream of a pressure regulator for fast response time. The *m/e* ratios were carefully selected to prevent interference from the fragmentation of parent species (18).

After reaching steady state for the $CO/D_2/C_2H_4$ reaction again for 30 min, another GC sample was taken for measuring the isotope effect on the steady-state rate of product formation. Then a step switch from D_2 to H_2 was introduced. Following the steady-state rate and transient measurements at a specified temperature, a bracketing reduction with flowing H_2 at 30 cm^3/min (19) was performed to maintain the activity of the catalyst. This bracketing reduction consisted of (i) heating the reactor to 573 K for 15 min, (ii) holding the reactor at 573 K for 30 min, and (iii) decreasing the temperature to reaction conditions over a 15-min time period.

RESULTS

Steady-State Measurements

Tables 1 and 2 report the turnover frequencies (TOF) for product formation for the $CO/H_2/C_2H_4$ and $CO/D_2/C_2H_4$ reaction over 4 wt% Rh/SiO_2 at 0.1 MPa and 483–573 K. The TOF for each product is defined as the rate of product formation (mole/s/g_{cat}) divided by the number of surface Rh atoms per gram of catalyst as measured by H_2 pulse chemisorption at 303 K. The $CO/H_2/C_2H_4$

TABLE 1

The Rate and Selectivity for Product Formation during the $CO/H_2/C_2H_4$ Reaction at 0.1 MPa

	Temperature			
	483 K	513 K	543 K	573 K
Product	TOF (s^{-1})*1000			
CH_4	0.18	0.17	0.18	0.21
C_2H_6	2.82	8.58	25.94	70.87
C_3H_6	0.40	0.16	0.15	0.25
1-C_4H_8	—	0.02	0.05	0.25
n-C_4H_{10}	—	0.05	0.04	0.34
i-C_4H_{10}	—	—	0.11	0.84
C_2H_5CHO	0.63	0.98	1.33	1.98
C_2H_4 conversion	0.61%	2.55%	6.95%	23.13%
	Selectivity			
$\frac{TOF_{C_2H_5CHO}}{TOF_{C_2H_6}}$	0.23	0.12	0.051	0.028

Note. $CO/H_2/C_2H_4/He = 30/30/30/30$ cm^3/min.

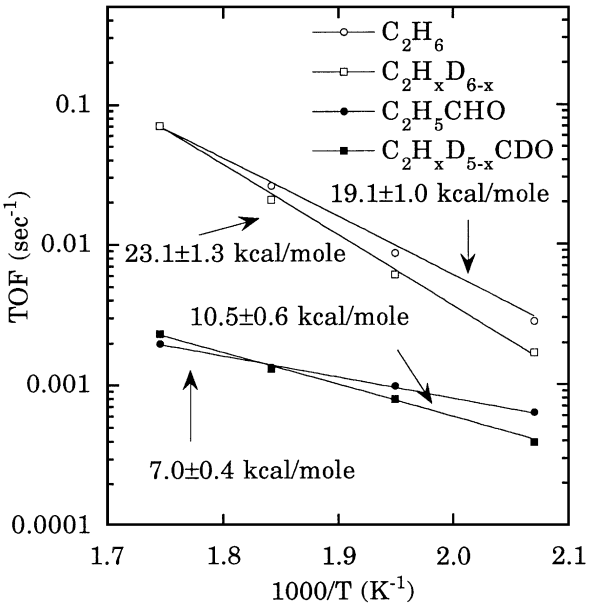

FIG. 3. Arrhenius plot of ethane and propionaldehyde formation on 4 wt% Rh/SiO_2 at 0.1 MPa for the $CO/H_2/C_2H_4/He$ and $CO/D_2/C_2H_4/He$ reaction systems, respectively.

reaction produced C_2H_6 and C_2H_5CHO as major products with trace amounts of methane, propylene, *n*-butane, and isobutane. The $CO/D_2/C_2H_4$ reaction produced deuterated ethane, propionaldehyde, methane, and $C_{3\text{-}4}$ hydrocarbons. The TOF listed for each species in Table 2 includes all the deuterated and nondeuterated species produced from the $CO/D_2/C_2H_4$ reaction. The extent of deuteration, location of deuterium on the molecule, and the concentration of each deuterated species were not determined. A separate deuterium pulse study shows that the extent of deuteration in both ethane and propionaldehyde increased with increasing temperature (18).

TABLE 2

The Rate and Selectivity for Product Formation during the $CO/D_2/C_2H_4$ Reaction at 0.1 MPa

	Temperature			
	483 K	513 K	543 K	573 K
Product	TOF (s^{-1})*1000			
CH_4	0.16	0.17	0.18	0.23
C_2H_6	1.69	6.05	20.79	70.93
C_3H_6	0.45	0.22	0.15	0.34
1-C_4H_8	—	0.01	0.05	0.37
n-C_4H_{10}	—	0.02	0.15	1.40
i-C_4H_{10}	—	—	—	—
C_2H_5CHO	0.39	0.79	1.30	2.33
C_2H_4 conversion	0.59%	2.50%	7.08%	22.96%
	Selectivity			
$\frac{TOF_{C_2H_5CHO}}{TOF_{C_2H_6}}$	0.23	0.13	0.063	0.033

Note. $CO/D_2/C_2H_4/He = 30/30/30/30$ cm^3/min.

The variation of TOF's with temperature is plotted in Arrhenius form in Fig. 3 for ethane and propionaldehyde. The activation energy for ethane and propionaldehyde was calculated to be 19.1 ± 1.0 and 7.0 ± 0.4 kcal/mole, respectively, in the $CO/H_2/C_2H_4$ reaction. The activation energy for deuterated ethane and deuterated propionaldehyde was calculated to be 23.0 ± 1.3 and 10.5 ± 0.6 kcal/mole, respectively, for the $CO/D_2/C_2H_4$ reaction. The $CO/H_2/C_2H_4$ results agree well with previous studies on Rh/SiO_2 (15, 20). The higher activation energies for the $CO/D_2/C_2H_4$ reaction reflect the presence of a normal deuterium isotope effect for the rate of formation of both ethane and propionaldehyde. The normal isotope effect is also evidenced by a value greater than one for the ratio of $\mathbf{r}_H$ to $\mathbf{r}_D$ listed in Table 3 ($\mathbf{r}_H$ is the rate of product formation from the reaction with hydrogen; $\mathbf{r}_D$ is the rate of product formation from the reaction with deuterium). Normal isotope effects are observed for ethane and propionaldehyde at all temperatures, except for an inverse isotope effect at 573 K for propionaldehyde formation. The inverse isotope effect observed for propionaldehyde occurs above the isotopic transition temperature, i.e., the temperature at which the rate of reaction with hydrogen is the same as with deuterium. For propionaldehyde formation this temperature is approximately 543 K and for ethane the temperature is approximately 573 K. The extent of the normal isotope effect (i.e., $\mathbf{r}_H/\mathbf{r}_D$) for both ethane and propionaldehyde formation increased as the reaction temperature decreased and moved away from the isotopic transition temperature. Extrapolation of the

TABLE 3

The Isotope Effect for Ethane and Propionaldehyde Formation

Temperature (K)	Isotope effect ($\mathbf{r}_H/\mathbf{r}_D$)	
	Ethane	Propionaldehyde
298	12.09[a]	—
483	1.66	1.61
513	1.42	1.24
543	1.25	1.02
573	1.00	0.85

Note. $\mathbf{r}_H$ is the rate of product formation during $CO/H_2/C_2H_4$ reaction.
$\mathbf{r}_D$ is the rate of product formation during $CO/D_2/C_2H_4$ reaction.
$CO/H_2/C_2H_4/He = 30/30/30/30$ cm^3/min.
$CO/D_2/C_2H_4/He = 30/30/30/30$ cm^3/min.
[a] Obtained from extrapolation of the Arrhenius curves in Fig. 3.

Arrhenius curve for C_2H_6 and $C_2H_xD_{6-x}$ to 298 K yields a value of 12.1, which is significantly greater than $\mathbf{r}_H/\mathbf{r}_D$ reported for ethylene hydrogenation on group VIII metals (7). The presence of CO in H_2/C_2H_4 appears to have a significant impact on the isotope effect.

Transient Responses

Figures 4a and 4b show the Ar, H_2, D_2, and HD transient responses to a step switch from H_2 to D_2 and from D_2 to H_2 while maintaining the steady-state CO and C_2H_4 flows over the catalyst at 0.1 MPa and 483 K. Hydrogen- and deuterium-containing ethylene and ethane responses are shown in Fig. 5. The rate of deuterated propionaldehyde formation was too low to give a smooth response curve. The inset in Fig. 4a shows the absolute MS intensity for H_2, D_2, and HD. The extent of the decrease in MS intensity for H_2 was significantly greater than that of the increase in MS intensity for D_2 as H_2 flow is switched to D_2 flow. Adjusting with the difference in ionization potentials (or response factors) between H_2 and D_2, the extent of the decrease in H_2 MS intensity is about the same as that of the increase for D_2. For comparison and modeling of transient responses for each species, the MS intensity response is normalized according to $[F(t) = C(t) - C^0]/[C^\infty - C^0]$, where C^0 = the initial concentration, C^∞ = the final concentration, and $C(t)$ = the concentration during the transient (21).

The intersection of the H_2 and D_2 curves at 0.5 in Fig. 4a indicates that H_2 is displaced by D_2 at a one-to-one correspondence and the total gaseous concentration of H_2 and D_2 remains constant during the switch. The step switch from H_2 to D_2 flow results in the replacement of adsorbed hydrogen by adsorbed deuterium. The lag of the H_2 curve as compared to the Ar curve is due to the adsorption and desorption of hydrogen. Adsorbed deuterium can: (i) desorb; (ii) substitute the adsorbed hydrogen to enter the reaction pathway, as shown in Fig. 2, to produce deuterium containing propionaldehyde, ethane, and ethylene; and (iii) combine with adsorbed hydrogen, desorbing as HD.

The HD response curve in Fig. 4a shows different features from those observed for H_2 to D_2 step switch during methanation (22), Fischer–Tropsch (23), and ammonia synthesis (24). The typical HD response curve in these reactions shows an initial increase to a maximum as deuterium flow is introduced. Then, the HD curve starts decreasing as adsorbed hydrogen on the catalyst surface gradually depletes. The HD response curve in Fig. 4a closely follows the D_2 curve even though all the adsorbed hydrogen from H_2 gaseous flow has depleted from the surface. The source of hydrogen for HD formation after replacement of H_2 by D_2 flow can be attributed to hydrogen produced from hydrogen/deuterium exchange on adsorbed ethyl following the classical Horiuti–Polanyi mechanism (7). Release of hydrogen from ethylene is also evidenced by early studies on deuteration of C_2H_4. These studies suggested that the rapid

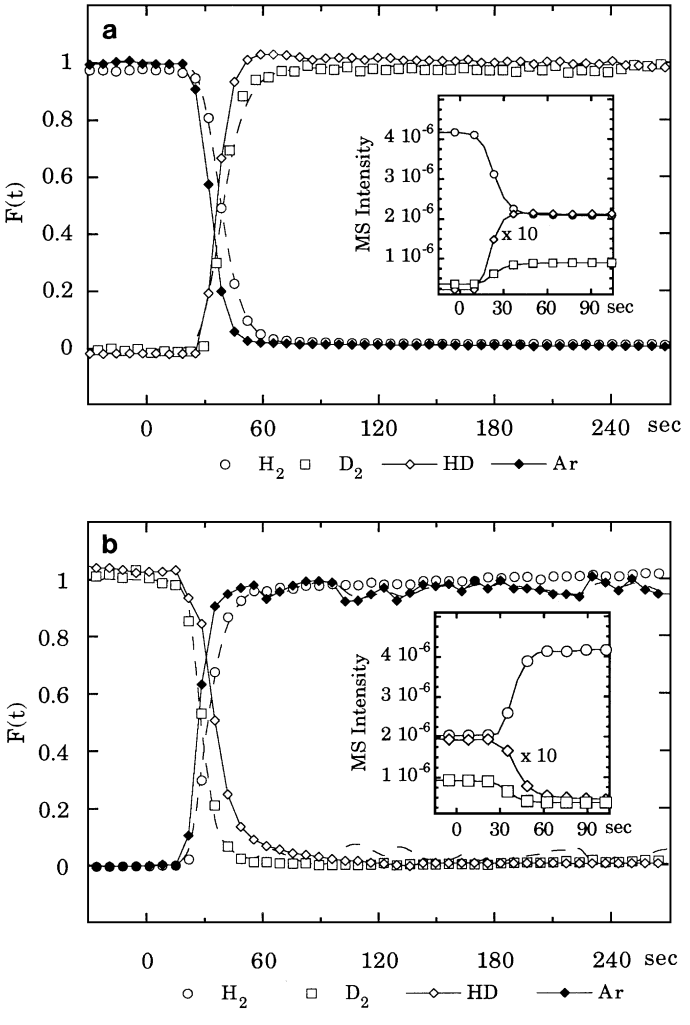

FIG. 4. (a) Transient response of HD to a H_2 to D_2 step switch at 483 K and 0.1 MPa. (b) Transient response of HD to a D_2 to H_2 step switch at 483 K and 0.1 MPa. (The dashed lines represent the model response.) Inset shows the absolute MS intensity as a function of time.

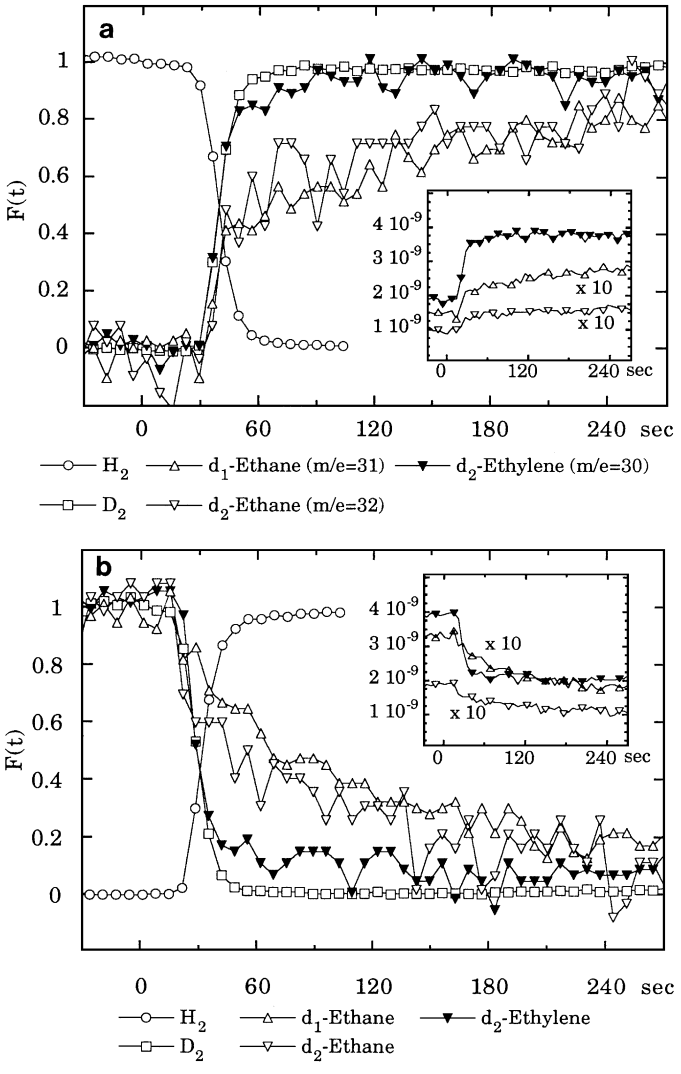

FIG. 5. (a) Transient responses of deuterated ethylene and ethane to a H_2 to D_2 step switch at 483 K and 0.1 MPa. (b) Transient responses of deuterated ethylene and ethane to a D_2 to H_2 step switch at 483 K and 0.1 MPa.

exchange between $*C_2H_5$ and *D provides adsorbed hydrogen for the initial hydrogenation of ethylene (7, 25, 26).

Tables 4 and 5 show the average residence times of H_2, D_2, and HD, and the deuterated propionaldehyde, respectively. The average residence time is calculated by

$$\tau_i = \int_0^\infty F_i(t)dt - \tau_{\mathrm{Ar}} \qquad [1]$$

where $F_i(t)$ is the normalized response of species i. The similar transport properties of Ar and those of H_2/D_2 lead to the assumption of the flow pattern of gaseous products being the same as that of Ar. Therefore, τ_i, the average residence time of surface intermediates leading to the gaseous products i is obtained by subtracting, τ_{Ar}, the average residence time of the Ar tracer through the reactor system, from $\int_0^\infty F_i(t)dt$ the average residence time for the product i (27). The HD response curve at 483 K led that of D_2 during the step switch from H_2 to D_2 while the HD response curve lagged that of D_2 during the step switch from D_2 to H_2. τ_{HD} during the switch from H_2 to D_2 is smaller than that during the switch from D_2 to H_2. The smaller τ_{HD} for the former case suggests that adsorbed hydrogen from C_2H_4 and hydrogen adsorption is readily available for combination with adsorbed deuterium as the step switch introduces deuterium flow to the catalyst. The larger value for τ_{HD} and the lagging of the HD response behind the D_2 response during the step switch from D_2 to H_2 suggest that the presence of a deuterium pool which slowly releases deuterium to react with the entering hydrogen.

Deuterium-containing C_2-hydrocarbon responses in Fig. 5 show that the $m/e = 30$, 31, and 32 increased during the step switch from H_2 to D_2 and decreased during the step switch from H_2 to D_2; $m/e = 30$ could be due to either d_2-ethylene or d_0-ethane. d_2-ethylene represents $C_2H_2D_2$ and d_0-ethane represents C_2H_6. d_i indicates the i number of deuterium atoms in the molecule. GC/MS analysis at 513 K showed d_2-ethylene contributed to 75% of $m/e = 30$ and d_0-ethane contributed to the rest during steady-state $CO/D_2/C_2H_4$ reaction. Thus, $m/e = 30$ is assigned to d_2-ethylene. Similarly, $m/e = 31$ can also be assigned to either d_3-ethylene and d_1-ethane. The GC/MS analysis showed that a 55% of $m/e = 31$ can be attributed to d_1-ethane. Assuming similar response factors, the inset in Fig. 5 shows that the d_2-ethylene was produced in much greater amounts than d_1- and d_2-ethane. The normalized responses show the d_2-ethylene response curve closely followed that of D_2, but significantly led that of d_1- and d_2-ethane, indicating that the exchange between ethylene and adsorbed deuterium was more rapid than the deuteration of ethylene to form d_1-ethane and d_2-ethane.

Figures 6a and 6b show the H_2, D_2, and HD responses to a H_2 to D_2 and D_2 to H_2 step switch, respectively, at 513 K. Comparison of the MS intensity of the HD response at 513 and 483 K shows that an increase in temperature increased

TABLE 4

The Average Residence Times, τ(s) of H_2, D_2, and HD Responses

	H_2	D_2	HD
	Step switch from H_2 to D_2		
483 K	5.96	7.17	2.94
513 K	5.80	6.16	6.69
543 K	6.33	6.76	6.85
	Step switch from D_2 to H_2		
483 K	6.36	2.60	9.38
513 K	7.46	2.76	4.31
543 K	6.75	6.85	6.45

TABLE 5

The Average Residence Times, τ, of the Propionaldehyde Responses

		d_0-propionaldehyde		d_1-propionaldehyde		d_2-propionaldehyde	
	θ	Eq. (1)	Model	Eq. (1)	Model	Eq. (1)	Model
			Step switch from H_2 to D_2				
513 K	0.0145	14.83	9.81	10.49	4.13	24.27	16.37
543 K	0.0340	25.58	24.45	10.05	1.10	22.57	16.84
573 K	0.0900	45.44	35.23	1.00	0.99	1.00	1.00
			Step switch from D_2 to H_2				
513 K	0.0408	41.65	31.26	62.51	51.60	14.49	10.30
543 K	0.0255	19.20	15.41	—	—	100.15	60.00
573 K	0.1119	56.50	44.75	183.46	121.31	75.33	51.48

— Not calculated.

the MS intensity of HD. The lead/lag relationship of HD, H_2, and D_2 responses at 513 K differs from those at 483 K. The HD response slightly lagged behind the D_2 response during the step switch from H_2 to D_2; the HD response initially led and then lagged behind that the D_2 during the step switch from D_2 to H_2, suggesting the presence of two deuterium pools with different rates of releasing deuterium to react with hydrogen.

Figures 7a and 7b show the d_2-ethylene and the d_1- and d_2-ethane responses to a H_2 to D_2 and D_2 to H_2 step switch, respectively at 513 K. The insets show the increased production of both d_2-ethylene, and d_1- and d_2-ethane as compared to 483 K. The normalized response shows the d_1- and d_2-ethane lagged behind the d_2-ethylene although they are closer to the D_2 response curve at 513 K than at 483 K. Although d_1-ethylene ($m/e = 29$) was not monitored, GC/MS analysis reveals that the amount of d_1-ethylene produced is 14 times more than that of d_2-ethylene during $CO/H_2/C_2H_4$ reaction. The trend of deuterium distribution in ethylene follows that of other catalysts (7) suggesting that hydrogenation of ethylene in this study follows the classical Horiuti–Polanyi mechanism.

Figures 8a and 8b show the deuterated propionaldehyde responses to a H_2 to D_2 and D_2 to H_2 step switches, respectively, at 513 K. The inset shows that d_1-, d_2-, and d_3-propionaldehyde increased their intensities to the same level. The normalized responses show that as the number of deuterium atoms incorporated in propionaldehyde increased, the delay time for their responses increased during the switch from H_2 to D_2. During the step switch from D_2 to H_2, the d_2- and d_3-propionaldehyde lead the d_1-propionaldehyde response.

Figure 8b also shows an immediate decrease followed by a sudden increase around 50 s, and then a gradual decay in the d_1-propionaldehyde response. The sudden increase of d_1-propionaldehyde may be attributed to the switch from deuteration of adsorbed d_0-acyl species to hydrogenation of

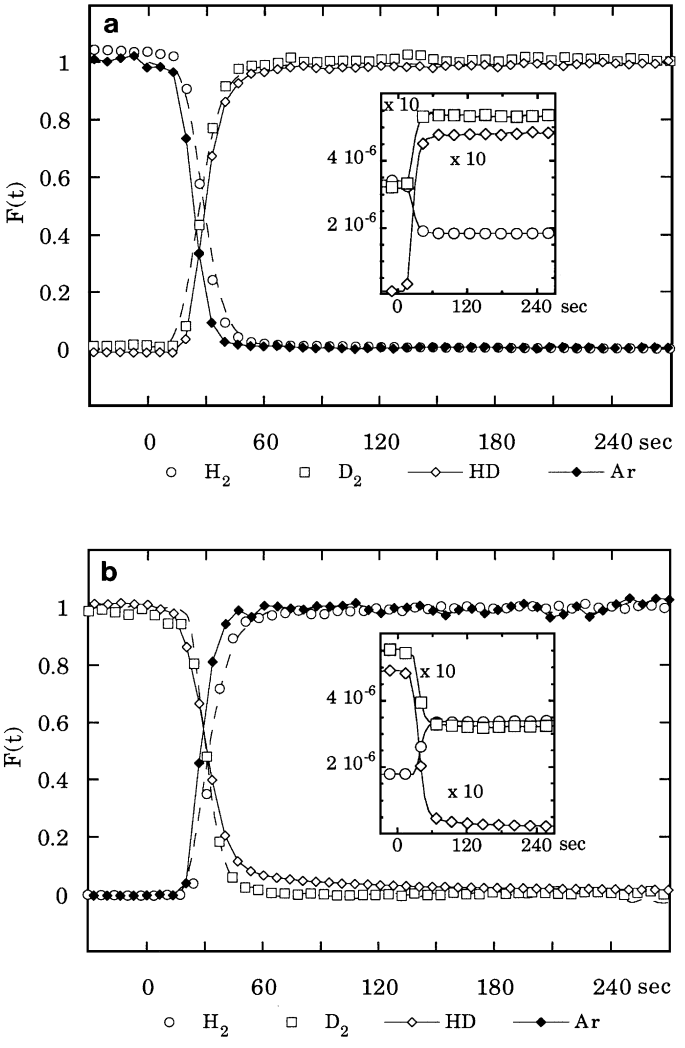

FIG. 6. (a) Transient response of HD to a H_2 to D_2 step switch at 513 K and 0.1 MPa. (b) Transient response of HD to a D_2 to H_2 step switch at 513 K and 0.1 MPa. (The dashed lines represent the model response.)

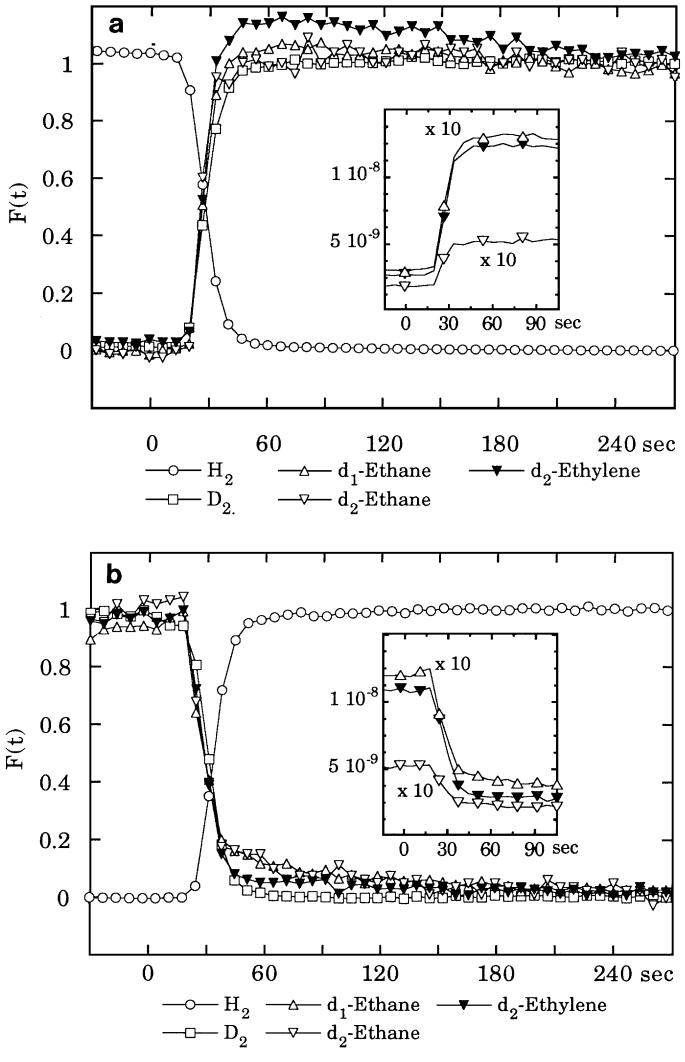

FIG. 7. (a) Transient responses of deuterated ethylene and ethane to a H_2 to D_2 step switch at 513 K and 0.1 MPa. (b) Transient responses of deuterated ethylene and ethane to a D_2 to H_2 step switch at 513 K and 0.1 MPa.

adsorbed d_1-acyl species. Figure 9 shows that both pathways II and III produce d_1-propionaldehyde. As deuterium flow is switched to hydrogen flow, depletion of adsorbed deuterium should cause a decrease in the rate of pathway II (the reaction of deuterium with the d_0-acyl species to produce d_1-propionaldehyde); an increase in concentration of adsorbed hydrogen may result in an increase in the rate of pathway III (the reaction of adsorbed hydrogen with the d_1-acyl species), causing a momentary rise in d_1-propionaldehyde response. A momentary increase in the rate of pathway III is possible if the significant increase in concentration of adsorbed hydrogen offsets the decrease in the concentration of the d_1-acyl species $*C_2H_4DCO$. Although d_1-acyl species response cannot be obtained directly from this study, its response may be deduced from the reaction mechanism. The d_1-acyl species would follow those of $*C_2H_4D$ and C_2H_5D, if the insertion of *CO into the $*C_2H_4D$ is not a rate-limiting step in the catalytic cycle for d_1-propionaldehyde formation. As the momentary increase in the rate of pathway III rapidly depleted the d_1-acyl species, the rate of pathway II continued its slow decay after 60 s. This slow decay, due to the slow deuteration of the d_0-acyl species, will be further discussed.

The IR response to both a H_2 to D_2 step switch and a D_2 to H_2 step switch at 513 K taken simultaneously with the MS response is shown in Fig. 10a. Gaseous CO at 2183 and 2106 cm^{-1} and linear CO at 2043 cm^{-1} were not altered during the step switch from H_2 to D_2 and D_2 to H_2. The major variation in the IR spectra is that a Si-OD peak at 2755 cm^{-1} (28, 29) developed and increased its intensity and the Si–OH around 3744 cm^{-1} decreased its intensity during the step switch from H_2 to D_2. The normalized IR intensity response of the Si-OD peak for both the H_2 to D_2 step and the D_2 to H_2 step switch at 513 K is plotted in Figs. 10b and 10c, respectively. The near symmetry in the Si-OD curve between the rise and decay curves reflects that the rate of spillover of adsorbed deuterium from the metal surface to

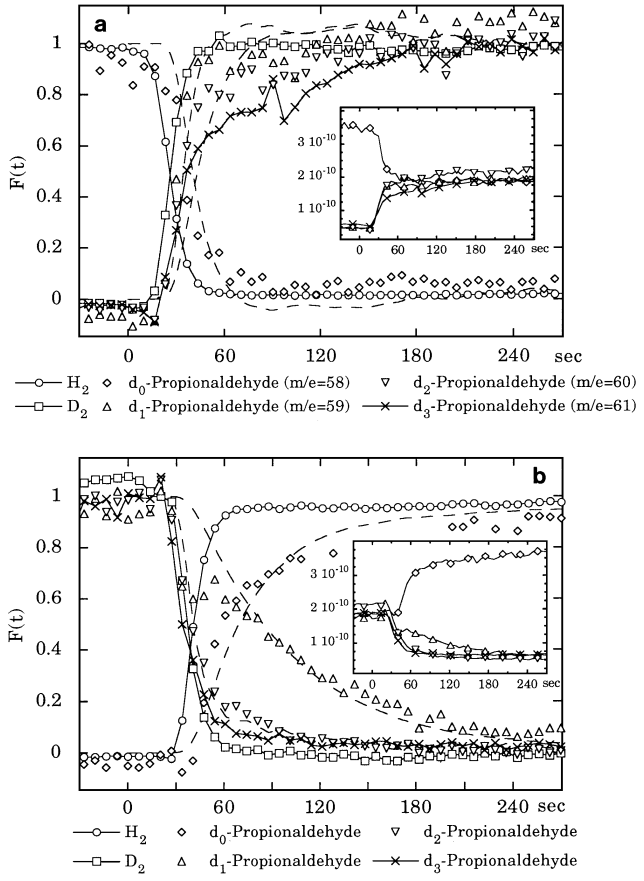

FIG. 8. (a) Transient responses of deuterated propionaldehyde to a H_2 to D_2 step switch at 513 K and 0.1 MPa. (b) Transient responses of deuterated propionaldehyde to a D_2 to H_2 step switch at 513 K and 0.1 MPa. (The dashed lines represent the model response.)

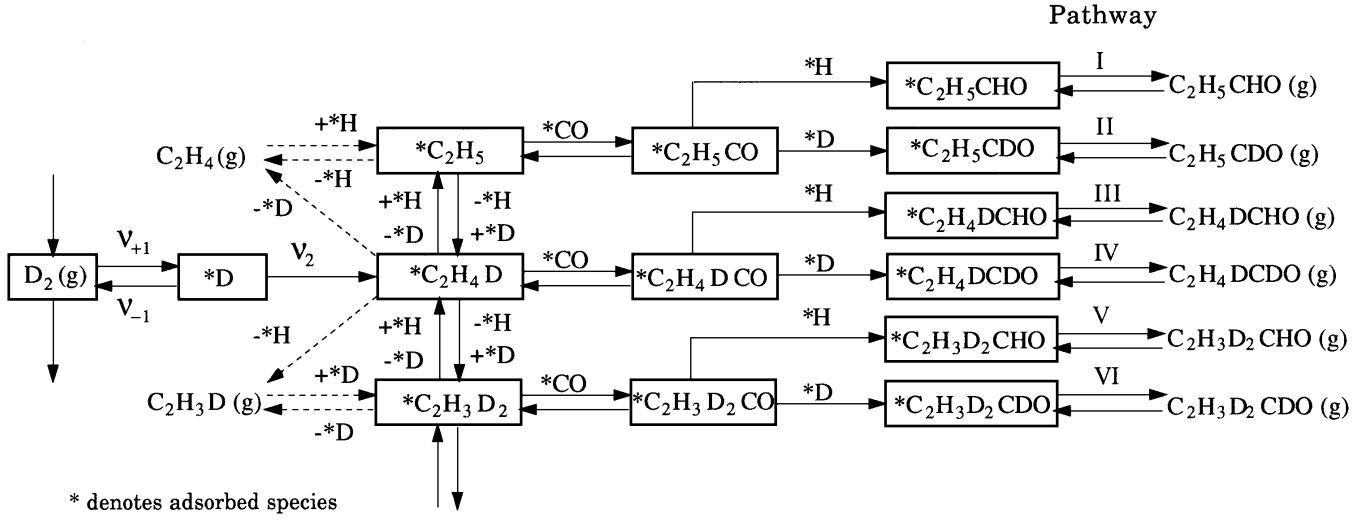

FIG. 9. Compartment model of H_2/D_2 tracing during ethylene hydroformylation.

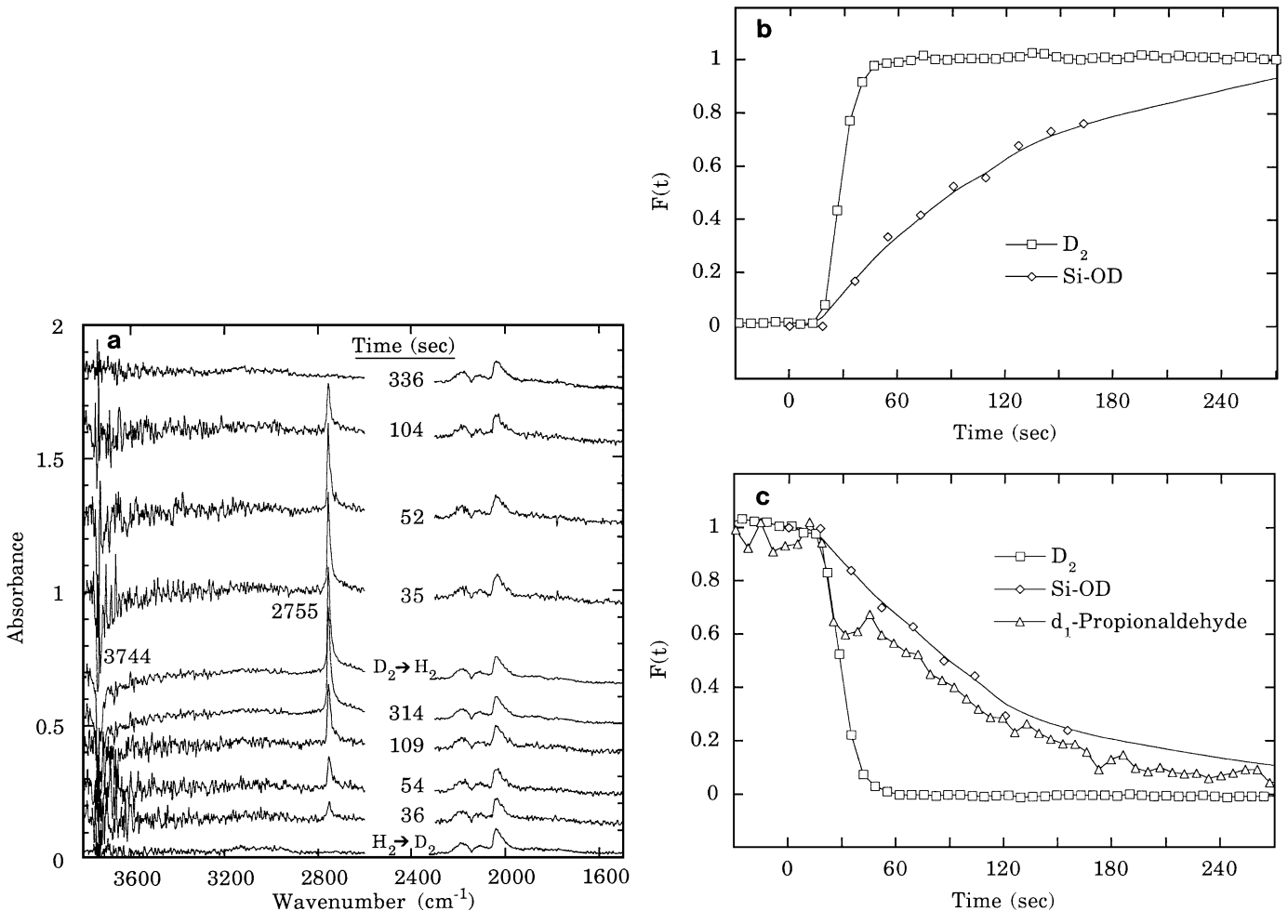

FIG. 10. (a) *In situ* IR spectra of heterogeneous hydroformylation on 4 wt% Rh/SiO_2 at 0.1 MPa and 513 K during H_2 to D_2 ($H_2 \rightarrow D_2$) and D_2 to H_2 ($D_2 \rightarrow H_2$) step switch. (b) Normalized *in situ* IR spectra of Si-OD peak compared to D_2 response during H_2 to D_2 step. (c) Normalized *in situ* IR spectra of Si-OD peak compared to D_2 and d_1-propionaldehyde response during D_2 to H_2 step.

the SiO_2 surface is about the same as that of the reverse spillover. The slow decay in the Si-OD response was found to be parallel to the response of d_1-propionaldehyde, shown in Fig. 10c, indicating that deuterium is available on the surface from reverse spillover for d_1-propionaldehyde formation long after gaseous D_2 has left the reactor. The low signal to noise ratio does not allow plotting of a well-defined Si-OH curve. The effect of Si-OH on the d_0-propionaldehyde response cannot be clearly determined. The decay of d_0-propionaldehyde is more rapid than those of d_1-propionaldehyde as shown in Fig. 8b. The hydrogen source for hydrogenation of acyl species appears to be more readily available for d_0-propionaldehyde formation than for d_1-propionaldehyde formation.

Figure 11 shows the deuterated ethylene and ethane responses led that of D_2 at 573 K. The insets show a significantly higher MS response for the deuterated ethylene and ethane. The large increase in MS intensity of the deuterated ethane responses with respect to temperature as compared to the d_2-ethylene response indicates that the exchange reaction leading to d_2-ethylene has a lower activation energy than the deuteration reaction producing deuterated ethane. The responses of deuterated ethylene and deuterated ethane overlapped and led the D_2 response.

Figure 12a shows the d_0-, d_1- and d_2-propionaldehyde responses at 573 K (d_3-propionaldehyde was not monitored at this temperature). d_1- and d_2-propionaldehyde closely followed that of D_2 while d_0-propionaldehyde lagged significantly behind H_2 during the H_2 to D_2 step switch. The smooth D_2/H_2 curve and the location of the intersection point indicate that both the H_2 to D_2 step switch and the D_2 to H_2 step switch were properly conducted and the steady-state flow condition was maintained. One conspicuous feature of the d_0-propionaldehyde response curve is a sudden increase in response upon D_2 entering the reactor, followed by a slow decay in the response. The latter may be due to the availability of the reverse spillover hydrogen that continues to hydrogenate the d_0-acyl species long after adsorbed hydrogen on the metal surface has been replaced by adsorbed deuterium. Figure 12b shows the d_2-propionaldehyde response is more rapid than d_0- and d_1-propionaldehyde responses during D_2 to H_2 step switch at 573 K. The profiles of d_0- and d_1-propionaldehyde response at 573 K resemble those at 513 K, but take a prolonged time to reach the steady state.

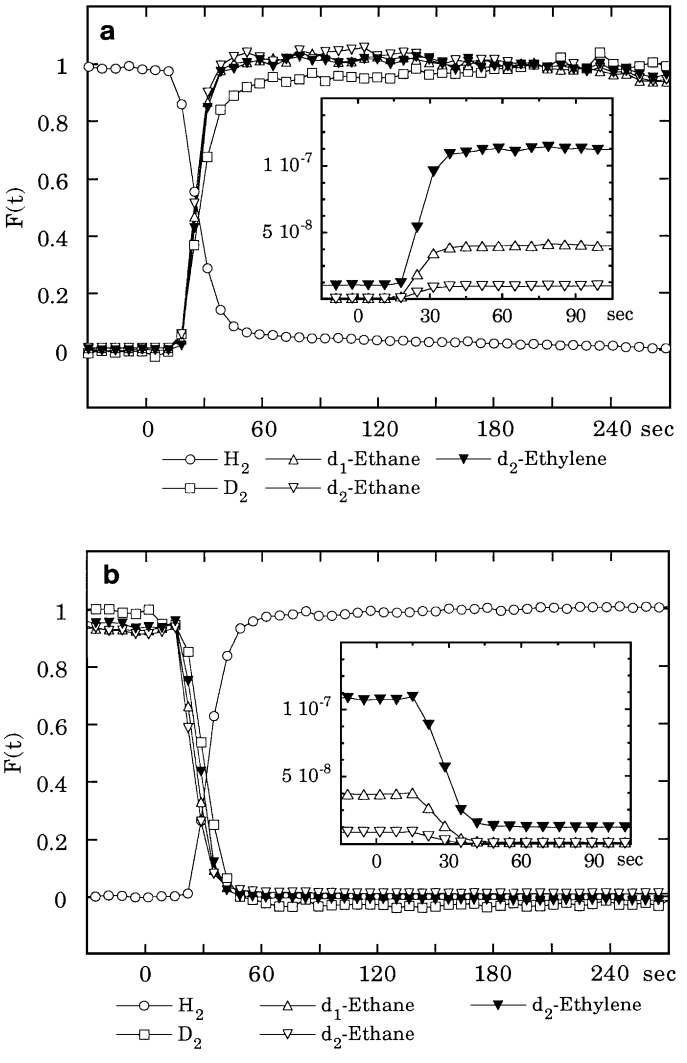

FIG. 11. (a) Transient responses of deuterated ethylene and ethane to a H_2 to D_2 step switch at 573 K and 0.1 MPa. (b) Transient responses of deuterated ethylene and ethane to a D_2 to H_2 step switch at 573 K and 0.1 MPa.

ANALYSIS OF TRANSIENT RESPONSE

Compartment Modeling of H_2 and D_2 Isotopic Transients

Figure 9 shows the proposed compartment model and reaction pathways for the formation of hydrogen- and deuterium-containing propionaldehyde from step injection of D_2. Exchange between C_2H_4 and adsorbed deuterium as well as deuteration/hydrogenation of C_2H_4 will not be modeled due to their rapid responses which do not provide clear resolution at temperatures above 483 K. Adsorbates distributed on the catalyst surface are lumped into boxes. Each species is considered well mixed in the pools (boxes) and the isotope-labeled species transfers from one pool to another according to the proposed mechanism. Detailed analysis of the concentration of each isotope-labeled species in the pool and their rates of transfer from these different pools is required to develop an understanding of the H_2/D_2 isotope effect of the transient responses. Transient responses of H_2 and D_2 carry mechanistic information for the adsorption of hydrogen, the first step of the reaction sequence. The rate of the forward and backward steps as well as the coverage of adsorbed hydrogen and deuterium can be obtained by modeling of the H_2/D_2 transient responses. Consider the

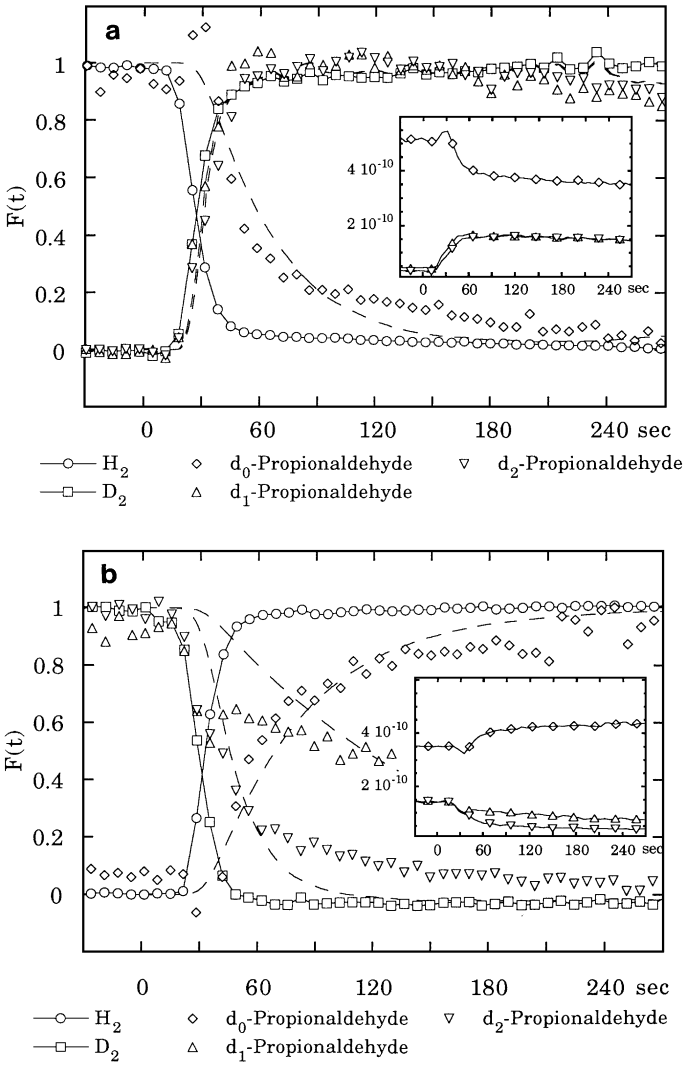

FIG. 12. (a) Transient responses of deuterated propionaldehyde to a H_2 to D_2 step switch at 573 K and 0.1 MPa. (b) Transient responses of deuterated propionaldehyde to a D_2 to H_2 step switch at 573 K and 0.1 MPa. (The dashed lines represent the model response.)

mole balances on the D_2 and the *D pools in Fig. 9:

$$\frac{dF_{D_2}}{dt} = \frac{Q^{in}_{D_2}}{VC_{D_2}} F^{in}_{D_2} + \frac{\upsilon_{-1d}\omega}{VC_{D_2}} F_{*D} - \left(\frac{\upsilon_{+1d}\omega - Q^{out}_{D_2}}{VC_{D_2}}\right) F_{D_2} \quad [2]$$

$$\frac{dF_{*D}}{dt} = \frac{\upsilon_{+1d}}{\theta_{*D}} F_{D_2} - \left(\frac{\upsilon_{-1d} + \upsilon_{2d}}{\theta_{*D}}\right) F_{*D}, \quad [3]$$

where:

F_{D_2} is the step transient response for D_2 (transient response of D_2).
$Q^{in}_{D_2}$ is the inlet molar flow rate of D_2 (2.232e-5 mole/s).
ω is the number of surface exposed Rh atoms (61 μmole Rh_{sites}/g_{cat}).
F_{*D} is the step transient response for *D (determined from modeling).
V is the volume of the IR cell (0.002 l).
C_{D_2} is the inlet concentration of D_2 (6.644e-3 mole/l).
$F^{in}_{D_2}$ is the inlet step transient of D_2 ($F^{in}_{D_2}$ equals to F_{Ar}).
υ_{-1d} is the rate of desorption of D_2 (determined from modeling).
υ_{+1d} is the rate of adsorption of D_2 (determined from modeling).
$Q^{out}_{D_2}$ is the outlet molar flow rate of D_2 (at differential conversion, $Q^{out}_{D_2}$ equals to $Q^{in}_{D_2}$).
θ_{*D} is the molar ratio of *D to the exposed Rh metal atom (determined from modeling).
υ_{2d} is the rate of D_2 incorporation into products (υ_{2d} equals to the steady-state rate of formation for all the deuterium-containing products except deuterated ethylene).

Note that the subscript d represents the rate of reaction involving deuterium. Equations [2] and [3] and the initial conditions at $t = 0$, $F_i = 0$ for all components contain all the information to describe the transient response of H_2/D_2 for any input function.

The parameters in Eqs. [2], [3] to be determined are θ_{*D}, υ_{+1d}, and υ_{-1d}. Considering the equations under steady state, Eq. [2] reduces to

$$\upsilon_{+1d} - \upsilon_{-1d} = \frac{Q^{in}_{D_2} - Q^{out}_{D_2}}{\omega} \quad [4]$$

and Eq. [3] reduces to

$$\upsilon_{+1d} = \upsilon_{-1d} + \upsilon_{2d}. \quad [5]$$

These equations reduce the number of unknown parameters to two. The values of the unknown parameters listed in Table 6 were obtained by fitting model response into the experimental response using the program TUTSIM (30). The model responses with the best fitted parameters are plotted in Figs. 4 and 6 to show the goodness of the fit. Fitting the H_2, D_2, and Ar response curves to Eqs. [2] and [3] produced the values for coefficients of F_{D_2} and F_{*D}. With a known value of the coefficients and υ_{2d}, υ_{+1d}, υ_{-1d} and θ_{*D} can be determined by Eq. [5].

The overlapping of the deuterated ethylene and ethane MS spectra does not allow simultaneous and continuous quantification of the rate of formation of d_1-, d_2-, d_3-, and d_4- ethylene as well as deuterated ethane during the step switch from H_2 to D_2 and D_2 to H_2. Only d_2-ethylene, d_1-, and d_2-ethane were monitored as a function of time. A separate GC/MS analysis was performed for steady-state $CO/D_2/C_2H_4$ reaction at 513 K. The results show that the rate of d_1-ethylene formation is 14 times greater than that of d_2-ethylene which is 10 times greater than the rate of conversion of ethylene to ethane and propionaldehyde and

TABLE 6

Rate Parameters for Hydrogen Adsorption/Desorption and Product Incorporation

	Step switch from H_2 to D_2		Step switch from D_2 to H_2		Isotope effect	
	H_2 (1)[a]	D_2 (2)[b]	H_2 (3)[a]	D_2 (4)[b]	(1)/(4)	(3)/(2)
483 K						
υ_{+1}[c]	0.8259	0.8903	1.3210	0.8218	1.01	1.48
υ_{-1}[c]	0.8224	0.8882	1.3176	0.8197	1.00	1.48
υ_2[c]	3.45e-3	2.08e-3	3.45e-3	2.08e-3	1.66	
θ[d]	0.1192	0.0977	0.1274	0.08721	1.45	1.30
513 K						
υ_{+1}	0.9842	1.3058	1.3386	0.8625	1.14	1.03
υ_{-1}	0.9747	1.2989	1.3291	0.8557	1.14	1.02
υ_2	9.56e-3	6.48e-3	9.56e-3	6.48e-3	1.40	
θ	0.1169	0.1244	0.1532	0.1012	1.16	1.23
513 K						
υ_{+1}	0.9842	1.3605	1.3386	0.9172	—	
υ_{-1}	0.9747	1.2989	1.3291	0.8557	—	
υ_2	9.56e-3	6.15e-2[e]	9.56e-3	6.15e-2[e]	—	
θ	0.1169	0.1296	0.1532	0.1077	—	
543 K						
υ_{+1}	1.1409	1.3339	1.3723	0.8975	1.27	1.02
υ_{-1}	1.1137	1.3168	1.3451	0.8805	1.27	1.02
υ_2	2.73e-2	1.71e-2	2.73e-2	1.71e-2	1.60	
θ	0.1310	0.1391	0.1615	0.1166	1.12	1.16
573 K						
υ_{+1}	1.3336	1.3713	1.4309	0.9858	1.35	1.04
υ_{-1}	1.2607	1.2980	1.3580	0.9126	1.38	1.05
υ_2	7.28e-2	7.33e-2	7.28e-2	7.33e-2	0.99	
θ	0.1361	0.1343	0.1949	0.1531	0.89	1.45

[a] The rate listed in columns 1 and 3 is for the reaction with H_2.
[b] The rate listed in columns 2 and 4 is for the reaction with D_2.
[c] The units of υ_{+1}, υ_{-1}, and υ_2 are (μmole/s/μmole Rh_{atom}).
[d] The units of θ are (μmole/μmole Rh_{atom}).
[e] υ_2 includes the rate of formation for deuterated ethylene.

their deuterated products. Including the rate of deuterated ethylene formation in υ_{2d} results in a slight increase in the deuterium coverage as shown in Table 6. Since the exclusion of the rate of deuterated ethylene formation in υ_{2d} does not lead to a significant error in estimation of hydrogen/deuterium coverages at 513 K, the rate of deuterated ethylene formation was not determined at 483 K, 543 K, and 573 K.

The isotope effect column in Table 6 is obtained by dividing the parameter for H_2 response during the H_2 to D_2 step by that for the D_2 response during the D_2 to H_2 step (column 1 divided by column 4), when both concentrations are decreasing. Another isotope effect can be obtained by dividing the parameters for the H_2 response during the D_2 to H_2 step by the D_2 response during the H_2 to D_2 step (column 3 divided by column 2), when both concentrations are increasing. At all temperatures the adsorption and desorption rates were much faster than the rate of incorporation into product, indicating this step is in quasi-equilibrium. The normal isotope effect on the coverage of adsorbed hydrogen decreased with increasing temperature.

Compartment Modeling of Deuterated Propionaldehyde Transients

Considering the pathway for the formation of C_2H_5CHO, replacement of H_2 by D_2 in a step model depletes the adsorbed hydrogen, resulting in a decrease in the formation of C_2H_5CHO. The response of C_2H_5CHO may be modeled by the mole balance involving $*C_2H_4CHO$ box shown in Fig. 9,

$$\theta_{*C_2H_5CHO}\frac{dF_{*C_2H_5CHO}}{dt} = \upsilon_{*C_2H_5CO}F_{*H}F_{*C_2H_5CO} - \upsilon_{*C_2H_5CHO}F_{*C_2H_5CHO}, \quad [6]$$

where:

$\theta_{*C_2H_5CHO}$ is the surface coverage of propionaldehyde.
$F_{*C_2H_5CHO}$ is the transient response of propionaldehyde.
$\upsilon_{*C_2H_5CHO}$ is the rate of formation of propionaldehyde.
F_{*H} is the transient response of adsorbed hydrogen, which is assumed to be the same as the H_2 response.
$F_{*C_2H_5CO}$ is the transient response of the adsorbed acyl species, which is assumed the same as the C_2H_5D response.
$\upsilon_{*C_2H_5CO}$ is the rate of formation of the adsorbed acyl species (at steady-state, $\upsilon_{*C_2H_5CO}$ is equal to $\upsilon_{*C_2H_5CHO}$).

By dividing all the terms by $\upsilon_{*C_2H_5CHO}$ and defining $\tau_{*C_2H_5CHO} = \theta_{*C_2H_5CHO}/\upsilon_{*C_2H_5CHO}$, Eq. [6] can be further rearranged for fitting model response to the experimental response as follows:

$$\tau_{*C_2H_5CHO}\frac{dF_{*C_2H_5CHO}}{dt} + F_{*C_2H_5CHO} = F_{*H}F_{*C_2H_5CO}. \quad [7]$$

The input (i.e., forcing) functions of the model equation are F_{*H} and $F_{*C_2H_5CO}$. The F_{*H} response is between the F_{H_2} and the F_{Ar} responses. Since the F_{H_2} response closely follows the F_{Ar}, F_{H_2} can be used for the F_{*H} response. The $F_{*C_2H_5CO}$ response cannot be obtained from transient IR due to the very weak signal and the inability to distinguish between adsorbed $*C_2H_5CO$ and $*C_2H_4DCO$ species. Assuming that CO insertion is in quasi-equilibrium permits the use of $F_{*C_2H_5D}$ as the input function for $F_{*C_2H_5CO}$ since the quasi-equilibrium would take place between $*C_2H_5$ and $*C_2H_5CO$ and the rapid deuteration allows $F_{*C_2H_5D}$ to follow $F_{*C_2H_5}$ very closely.

Table 5 presents the average residence times obtained by fitting the transient response curves by the above equation. Comparing the model results from Eq. [7] with

those obtained from Eq. [1], the d_0-propionaldehyde results agree within the experimental error. The d_1- and d_2-propionaldehyde results are listed for comparison. The model of Eq. [7] does not fully describe the dynamics of d_1- and d_2-propionaldehyde formation which involves two pathways, as shown in Fig. 9. Modeling of these responses with two pathways involves too many adjustable parameters to produce meaningful results.

DISCUSSION

The salient features of the transient responses of D_2, H_2, and deuterated and hydrogenated product responses include the asymmetrical responses between hydrogen- and deuterium-containing product responses, deuterated C_2 hydrocarbon responses closely following that of D_2 at temperatures above 483 K, and all the deuterated propionaldehyde responses lagging behind those of deuterated ethylene and ethane. These unique features provide qualitative information on the reaction mechanism. The asymmetrical response is a manifestation of the H_2/D_2 isotope effect on the rate of formation for deuterated and hydrogenated products. The close response between D_2 and deuterium-containing ethylene and ethane suggests a high rate of hydrogenation/deuteration and low residence time of intermediates leading to the formation of ethane. The significant lag in the deuterated propionaldehyde response compared to those of D_2 and deuterium-containing hydrocarbons reflects the time required for deuterium to travel from adsorbed deuterium to gaseous deuterated propionaldehyde in the reaction pathway shown in Fig. 9. The delay in propionaldehyde response may result from one of these steps, i.e., CO insertion, hydrogenation of acyl intermediates, or desorption of adsorbed propionaldehyde.

If desorption of propionaldehyde were the rate-limiting step, an increase in temperature would increase the rate of desorption, resulting in a significant decrease in the residence time of intermediates leading to deuterated propionaldehyde. Since the residence time of intermediates leading to deuterated propionaldehyde did not decrease with increasing temperature, desorption of propionaldehyde can be ruled out as the rate-limiting step. SSITKA with $^{13}CO/CO$ pulse switch on the same catalyst used in this study shows that increasing hydrogen partial pressure decreases the residence of adsorbed acyl species (15). The rate as a function of partial pressure of reactant is best fit by the LHHW (Langmuir–Hinshelwood–Hougen–Watson) kinetic model with hydrogenation of the acyl species as the rate-limiting step. The LHHW kinetic model can be expressed as

$$\mathrm{TOF}_{C_2H_5CHO} = \frac{k_6 K_1 K_2 K_3 K_4 K_5 P_{CO} P_{H_2} P_{C_2H_4}}{\left(1 + K_2 P_{CO} + \sqrt{K_1 P_{H_2}} + K_3 P_{C_2H_4}\right)^2}, \quad [8]$$

where all the k_i and K_i's are defined in Fig. 2. Considering the isotope effect for propionaldehyde formation,

$$\frac{\mathrm{TOF}_{C_2H_5CHO}}{\mathrm{TOF}_{d\text{-}C_2H_5CHO}} = \left(\frac{k_{6h} K_{1h} K_{4h}}{k_{6d} K_{1d} K_{4d}}\right) \times \left(\frac{1 + K_2 P_{CO} + \sqrt{K_{1d} P_{D_2}} + K_3 P_{C_2H_4}}{1 + K_2 P_{CO} + \sqrt{K_{1h} P_{H_2}} + K_3 P_{C_2H_4}}\right)^2, \quad [9]$$

where K_{1h} is the hydrogen adsorption equilibrium constant, K_{1d} is the deuterium adsorption equilibrium constant, K_{4h} is the ethylene partial hydrogenation equilibrium constant, K_{4d} is the ethylene partial deuteration equilibrium constant, k_{6h} is the rate constant for hydrogenation of the acyl species, and k_{6d} is the rate constant for deuteration of the acyl species. K_2, K_3, and K_5 are the equilibrium parameters which are not affected by the H_2/D_2 isotope effect. These parameters are canceled when the ratio is taken.

The equilibrium isotope effect for hydrogen/deuterium chemisorption, K_{1h}/K_{1d}, may be obtained from comparison of coverage and residence time of adsorbed hydrogen and deuterium. Considering the hydrogen adsorption step, $H_2 + 2^* \Leftrightarrow 2^*H$, in equilibrium (15), an equilibrium constant for hydrogen adsorption can be defined as

$$K_{1h} = \frac{\theta_{*H}^2}{P_{H_2} \theta_v^2}, \quad [10]$$

where θ_{*H} is the surface coverage of hydrogen, P_{H_2} is the hydrogen pressure, and θ_v is the vacant sites on the catalyst surface. The lack of information on the effect of H_2 and D_2 adsorption on the vacant sites leads to the proposition that adsorption/desorption of H_2 and D_2 does not vary θ_v. Thus, dividing K_{1h} by a similarly defined K_{1d} gives a relationship relating the ratio of adsorption equilibrium constant to the ratio of surface coverage:

$$\frac{K_{1h}}{K_{1d}} = \frac{\theta_{*H}^2}{\theta_{*D}^2}. \quad [11]$$

The values of K_{1h}/K_{1d} values ranged from 2.1 at 483 K to 1.34 at 543 K and 0.79 at 573 K, indicating a normal isotope effect for hydrogen adsorption. The thermodynamic isotope effect on hydrogen/deuterium chemisorption has been previously discussed and estimated on Ru and Ni supported catalysts (7). It was conclude that K_{1h}/K_{1d} was greater than one under the Fischer–Tropsch reaction conditions between 453 and 498 K.

Plugging the appropriate values into Eq. [9] for propionaldehyde formation at 513 K, where $\mathrm{TOF}_{C_2H_5CHO}/\mathrm{TOF}_{d\text{-}C_2H_5CHO}$ is the isotope effect calculated for the formation of propionaldehyde from the steady-state GC rate found in Table 3, K_{1h}/K_{1d} is determined from Eq. [11] using the fitted values in Table 6, and k_{6h}/k_{6d} is determined from the residence times in Table 5, reveals K_{4h}/K_{4d} to be 1.32. The presence of a normal isotope effect on the partial

hydrogenation of C_2H_4 is highly possible. One major discrepancy in combining the results of transient and steady-state kinetics is that k_6 obtained from the transient response accounts for the reverse spillover of hydrogen while the steady-state kinetic model only considers the adsorbed hydrogen on the Rh surface.

Comparison of the decay of deuterated propionaldehyde response at 513 K (Fig. 8b), 543 K (not shown here), and 573 K (Fig. 12b) during step switch from D_2 to H_2 shows that the d_1-propionaldehyde response always lagged behind those of d_2- and d_3-propionaldehyde. The parallel responses of Si-OD and d_1-propionaldehyde lead to the proposition that the reverse spillover deuterium from Si-OD is the source of deuterium for deuteration of the d_0-acyl species long after adsorbed deuterium of the Rh surface has been replaced by adsorbed hydrogen. The lack of impact of the reverse spillover deuterium on d_2- and d_3-propionaldehyde indicates that these species are rapidly removed from the catalyst surface by reaction with adsorbed hydrogen and that d_1- and d_2-acyl species do not have access to the reverse spillover deuterium from Si-OD.

The d_1-acyl and d_2-acyl species are produced from CO insertion into $*C_2H_4D$ and $*C_2H_3D_2$ of which formation involves deuteration and exchange reactions, probably taking place primarily on the metal surface. Early work by Horiuti and Polanyi on ethylene hydrogenation on Ni proposed a highly reversible half-hydrogenation step (26). Recent studies have also suggested a rapid hydrogen and deuterium exchange on the alkyl backbone on Ru surface (11). The easy accessibility of the d_0-acyl species to Si-OD suggest that the d_0-acyl species may be located near the interface between metal particle and oxide support. The interface between the support and metal has also been proposed as the site for CO insertion to produce the acyl intermediate (31).

The isotope effect on hydrogenation/deuteration of the adsorbed acyl and deuterated acyl species can be illustrated by comparing the d_0- and d_1-propionaldehyde responses, as well as the d_1- and d_2-propionaldehyde responses in Fig. 8. The isotope effect for ($*C_2H_5CO + *H \rightarrow *C_2H_5CHO$) and ($*C_2H_5CO + *D \rightarrow *C_2H_5CDO$) can be examined qualitatively by comparing d_0-propionaldehyde response in Fig. 8a and d_1-propionaldehyde response in Fig. 8b. In both cases, hydrogen and deuterium concentrations are decreasing. However, $*C_2H_5CO$ is decreasing for d_0-propionaldehyde in Fig. 8a while $*C_2H_5CO$ is increasing for d_1-propionaldehyde in Fig. 8b. The higher concentration of $*C_2H_5CO$ should accelerate the rate of deuteration to form d_1-propionaldehyde. However, the normal isotope effect appears to significantly decrease the rate of reaction with deuterium leading to the slower response for d_1-propionaldehyde. Similar observations for the isotope effect on the hydrogenation/deuteration were obtained for the d_1-acyl species by comparing the d_1-propionaldehyde ($*C_2H_4DCO + *H \rightarrow *C_2H_4DCHO$) in Fig. 8a with the d_2-propionaldehyde ($*C_2H_4DCO + *D \rightarrow *C_2H_4DCDO$) in Fig. 8b. The same kind of isotope effect was also observed for the d_2-acyl species. Although lack of data on the rate of formation of each deuterated propionaldehyde prohibits quantification of the isotope effect, comparison of the transient responses of deuterated products allows observation of the significant normal isotope effect for hydrogenation/deuteration of d_0-, d_1-, and d_2-acyl species.

CONCLUSIONS

The steady-state rate of product formation as well as the transient responses of H_2, D_2, hydrogen- and deuterium-containing products to a step switch from H_2 to D_2 and from D_2 to H_2 has been determined for $CO/H_2/C_2H_4$ and $CO/D_2/C_2H_4$ reactions over 4 wt% Rh/SiO_2 at 483–573 K and 0.1 MPa. A normal isotope effect is observed for the steady-state rate of formation for ethane and propionaldehyde, chemisorption of hydrogen/deuterium, hydrogen/deuterium coverage, hydrogenation/deuteration of adsorbed acyl species. The normal isotope effect for hydrogenation of the adsorbed acyl species supports the step as the rate-limiting step. *In situ* IR of Si-OD and C_2H_5CHO responses indicates that the reverse spillover deuterium participates in deuteration of adsorbed d_0-acyl species. The easy accessibility of Si-OD's deuterium to the adsorbed acyl species suggests that the d_0-acyl species may be located near the $Rh\text{-}SiO_2$ interface.

The significant difference in response between deuterated ethane and deuterated propionaldehyde reflects the different nature of either adsorbed deuterium or active sites for deuteration of adsorbed ethyl and acyl species. These differences provide the possibility of selective poisoning of deuteration/hydrogenation of adsorbed ethyl species without considerably suppressing deuteration/hydrogenation of adsorbed acyl species.

REFERENCES

1. Tamaru, K., Dynamic relaxation methods in heterogeneous catalysis *in* "Catalysis: Science and Technology" (J. Anderson and M. Boudart, Eds.), Vol. 9, p. 87. Springer-Verlag, Berlin/Heidelberg/New York, 1991.
2. Dumesic, J., Rudd, D., Aparicio, L., Rekoke, J., and Trevino, A., "The Microkinetics of Heterogeneous Catalysis." Am. Chem. Soc. Washington, DC, 1993.
3. Happel, J., "Isotopic Assessment of Heterogeneous Catalysis." Academic Press, New York, 1986.
4. Tanaka, K.-I., *Adv. in Catal.* **33**, 99 (1985).
5. Davis, S., Gillespie, G., and Somorjai, G., *J. Catal.* **83**, 131 (1983).
6. Kellner, C. S., and Bell, A., *J. Catal.* **67**, 175 (1981).
7. Ozaki, A., "Isotopic Studies of Heterogeneous Catalysis." Academic Press, New York, 1977.
8. Emmit, P., *Catal. Rev.* **7**(1), 1 (1972).
9. Bond, G. C., Philipson, J., Wells, P., and Winterbottom, J., *Trans. Faraday Soc.* **62**, 443 (1966).
10. Rooney, J., and Webb, G., *J. Catal.* **3**, 488 (1964).
11. Shannon, S., and Goodwin, J., Jr., *Chem. Rev.* **95**, 677 (1995).

12. Biloen, P., *J. Mol. Catal.* **21**, 17 (1983).
13. Melander, L., and Saunders, W., "Reaction Rates of Isotopic Molecules." Wiley, New York, 1980.
14. Cornils, B., Hydroformylation, *in* "New Synthesis with Carbon Monoxide" (J. Falbe, Ed.). Springer-Verlag, New York, 1980.
15. Balakos, M. W., and Chuang, S. S. C., *J. Catal.* **151**, 266 (1995).
16. Chuang, S. S. C., and Pien, S., *J. Catal.* **135**, 618 (1992).
17. Chuang, S. S. C., Brundage, M. A., Balakos, M., and Srinivas, G., *Appl. Spectrosc.* **49**(8), 1151 (1995).
18. Brundage, M. A., M.S. thesis, The University of Akron, 1994.
19. Sen, B., and Vannice, M. A., *J. Catal.* **113**, 52 (1988).
20. Balakos, M. W., and Chuang, S. S. C., *J. Catal.* **151**, 253 (1995).
21. Balakos, M. W., Chuang, S. S. C., Srinivas, G., and Brundage, M. A., *J. Catal.* **157** (1995).
22. Happel, J., Cheh, H., Otarod, M., Ozawa, S., Severdia, A., and Yoshida, T., *J. Catal.* **75**, 314 (1982).
23. Zhang, X., Ph.D. dissertation, The University of Pittsburgh, 1986.
24. Nwalor, J., Goodwin, J. G., Jr., and Biloen, P., *J. Catal.* **117**, 121 (1989).
25. Turkevich, J., Schissler, D., and Irsa, P., *J. Phys. Colloid Chem.* **55**, 1078 (1951).
26. Keii, T., *J. Res. Inst. Catal. Hokkaido Univ.* **3**, 35 (1953).
27. Srinivas, G., Chuang, S. S. C., and Balakos, M. W., *AIChE J.* **39**, 530 (1993).
28. Hair, M. L., "Infrared Spectroscopy in Surface Chemistry," p. 83. Dekker, New York, 1967.
29. Conner, W. C., Jr., Spillover of Hydrogen, *in* "Hydrogen Effects in Catalysis" (Z. Paal and P. Menon, Eds.), p. 332. Dekker, New York, 1988.
30. Reynolde, W., and Wolf, J., "TUTSIM Block Diagram Language," TUTSIM Products, Palo Alto, CA, 1991.
31. van der Berg, F. G. A., Ph.D. dissertation, University of Leiden, The Netherlands, 1983.